Polymer Chemistry

PAPER

View Article Online
View Journal | View Issue

Cite this: *Polym. Chem.*, 2019, **10**, 5103

Expanding the monomer scope of linear and branched vinyl polymerisations *via* copper-catalysed reversible-deactivation radical polymerisation of hydrophobic methacrylates using anhydrous alcohol solvents†

Sean Flynn, Andrew B. Dwyer, Pierre Chambon and Steve Rannard *

Cu-Catalysed reversible-deactivation radical polymerisation of hydrophobic methacrylate monomers in anhydrous alcohols has been expanded to explore the scope of this unusual choice of solvent. A range of linear methacrylic homopolymers with well-targeted molecular weight and low dispersity ($Đ$ = 1.12–1.53) have been generated in anhydrous methanol and isopropanol with relative ease. These solvents are normally considered antisolvents and employed to precipitate such polymers; therefore, our studies have assessed the polymerisation reaction mixture homogeneity and extent of reaction control. Statistical copolymerisations with the bi-functional monomer, ethylene glycol di-methacrylate (EGDMA), has led to branched statistical copolymers with weight average molecular weights up to M_w = 1.76 × 10^6 g mol^{-1}; subsequent triple-detection size exclusion chromatography studies have provided insight into the impact of monomer structure on the extent of branching within the final isolated polymers. The ability to control branched copolymer molecular weights under these conditions through variation of EGDMA concentrations was seen to be highly dependent on methacrylate monomer chemistry. A number of factors which are likely to effect branching reactions during the polymerisation of hydrophobic methacrylates in anhydrous alcohols are discussed.

Received 28th May 2019,
Accepted 10th August 2019

DOI: 10.1039/c9py00777f

rsc.li/polymers

Introduction

The ability to direct polymerisation processes and influence polymer properties such as molecular weight, dispersity, functionality and macromolecular architecture is an ongoing challenge for research groups globally.[1–4] The discovery of reversible-deactivation radical polymerisation (RDRP) techniques represents perhaps the most significant recent step towards controlling radical polymerisation processes and has had a considerable impact on the advances made in materials chemistry over the last quarter of a century.

Since the first "living" radical polymerisation was reported by Otsu *et al.*[5] in 1982, a number of RDRP techniques have emerged including: nitroxide-mediated polymerisation,[6–9] atom-transfer radical polymerisation,[10,11] iodine degenerative transfer polymerisation,[12,13] reversible addition–fragmentation chain transfer polymerisation[14] and single electron transfer-living radical polymerisation (SET-LRP).[15] Whilst the detailed mechanistic aspects of each technique are undoubtedly unique, they commonly equip polymer chemists with the ability to polymerise a wide range of monomers with a level of control to dictate the number of growing chains thus allowing for the generation of polymers with pre-determined number average molecular weight (M_n) whilst maintaining relatively low dispersity between polymer chains ($Đ$ = 1.01–1.30).

The level of control provided by RDRP techniques has permitted the generation of numerous novel macromolecular architectures including: block copolymers,[16–18] multi-block copolymers,[19–27] star polymers,[27–33] branched polymers[34–38] and hyperbranched polymers.[39–44] One approach which relies heavily on the ability to control the number of propagating polymer chains to avoid the formation of an insoluble gelled network is the generation of branched polymers *via* statistical copolymerisation of mono- and bifunctional monomers (BFM).[45] The mechanism of branched polymer architecture formation, and the branching processes occurring during copolymerisation, are well understood;[46–50] consequently, this approach has been used to generate branched polymers using

Materials Innovation Factory, University of Liverpool, Crown Street, L69 7ZD, UK. E-mail: srannard@liv.ac.uk

†Electronic supplementary information (ESI) available: Experimental details, NMR spectra, TD-SEC analyses, additional figures and calculations. See DOI: 10.1039/c9py00777f

a range of different RDRP techniques.[51–57] Branched polymers synthesised in this way consist of multiple primary chains conjoined into a distribution of branched macromolecular architectures, consisting of different numbers of primary chains and reflecting the statistical nature of BFM incorporation. As a result, samples typically contain high molecular weight fractions and broad molecular weight distributions. Many factors can influence the prevalence of branching reactions during polymerisation; the feedstock ratio of BFM to initiator ($[B]_0/[I]_0$) determines the fraction of polymer chains theoretically capable of partaking in branching reactions,[58] whilst the statistical distribution of BFM is also dependent on the level of electronic interaction between co-monomers.[59,60] The inclusion of BFM into the polymer structure, whether *via* intermolecular branching or intramolecular cyclisation, impacts the extent of branching and may also be heavily influenced by the concentration at which polymerisations are conducted.[61–64] These factors must always be considered when designing new branching copolymerisation reactions using this approach.

Recently, there has been increasing interest in the RDRP of monomers within reaction media typically considered as bad solvents for the resulting polymer; many strategies have been developed to overcome polymer–solvent incompatibility. For example, Percec and co-workers have demonstrated the ability to conduct SET-LRP of hydrophobic monomers in biphasic reaction mixtures to generate linear homopolymers of low dispersity with considerable control over molecular weight.[65–70] Additionally, polymerisation-induced self-assembly has become established over recent years, facilitating the formation of amphiphilic block copolymers in solvents which are incompatible with one copolymer block segment;[71] growth of a solvent-incompatible secondary block drives the self-assembly of propagating polymer chains to form well-defined, sterically-stabilised block copolymer nanoparticles of varying size and morphology.[72–76] Alternatively, Gao and co-workers have used emulsion polymerisation to generate high molecular weight hyperbranched polymers *via* self-condensing vinyl polymerisation of water-immiscible acrylic and methacrylic inimers in aqueous emulsion.[77,78] Compartmentalisation of inimers within emulsion droplets has proved an effective technique to promote the formation of materials with higher molecular weights and greater degrees of branching than those produced in solution.[79]

We have previously reported the highly controlled nature of the Cu-catalysed RDRP of *n*-butyl methacrylate (*n*BMA) at elevated temperature in anhydrous methanol (MeOH; generally considered a poor solvent for the resulting polymer), to give poly(*n*BMA) of controlled molecular weight and low dispersities ($Đ$ = 1.03–1.10).[80] This technique has been used to generate various p(*n*BMA) architectures including: linear homopolymers, AB block copolymers, ABA triblock copolymers, branched statistical copolymers, branched statistical block copolymers and hyperbranched polydendrons.[81,82] Herein, we present our most recent work which expands the scope of hydrophobic monomers that can be polymerised *via* Cu-catalysed RDRP in anhydrous alcohol solvents. Pyrene fluorescence emission spectroscopy has been utilised to assess the relative polarity of homogeneous alcohol polymerisation mixtures across a range of methacrylate monomers and related to the controlled nature of Cu-catalysed RDRP in anhydrous methanol or isopropyl alcohol (IPA) during the formation of numerous polymer architectures including linear homopolymers and branched statistical copolymers. In cases where polymerisation-induced phase separation is observed during the reaction, the influence of polymerisation homogeneity on the controlled reaction is studied and its impact on the branched statistical copolymerisation is discussed.

Results and discussion

Evaluating monomer impact on polymerisation mixture polarity

The effect of monomer upon the solution properties of a polymerisation mixture is often an overlooked factor when designing new polymerisation reactions, especially those conducted at high solids content. Following our previous reports which demonstrated the ability to polymerise *n*BMA at concentrations up to 50 weight percent (wt%) solids content in anhydrous MeOH,[80,82] the impact of a wide range of hydrophobic methacrylate monomers on the reaction solvent quality was evaluated. Methyl methacrylate (MMA), ethyl methacrylate (EMA), *n*-butyl methacrylate, *tert*-butyl methacrylate (*t*BMA), *n*-hexyl methacrylate (*n*HMA), cyclohexyl methacrylate (CHMA), benzyl methacrylate (BzMA), 2-ethyl hexyl methacrylate (EHMA), lauryl methacrylate (LMA) and stearyl methacrylate (SMA) were selected as a series of hydrophobic methacrylate monomers for this study with linear and branched aliphatic side chains ranging from 1 to 18 carbons and aromatic and aliphatic cyclic structures. To establish the feasibility of using these monomers in Cu-catalysed RDRP in anhydrous alcohols, the miscibilities of representative monomer–alcohol mixtures (50 wt%) were investigated (ESI, Table S1a†). Monomer–MeOH miscibility was assessed visually and showed homogeneous mixtures for all monomers under conditions representative of Cu-catalysed RDRP, with the exception of SMA; at ambient temperature ($<T_m$ SMA) SMA remained an insoluble white powder in MeOH which formed a biphasic mixture upon heating above 20 °C (ESI, Fig. S1a†). Homogeneous monomer–IPA solutions were formed for all monomers at both ambient and elevated temperatures (ESI, Table S1b, Fig. S1b†).

Monomer–alcohol mixture polarities were assessed using fluorometric analysis by examination of the fine structure of the fluorescence emission spectrum of pyrene, dissolved in monomer and monomer–alcohol mixtures (Fig. 1). This technique is commonly used for comparison of organic solvent polarities and to determine the critical micelle concentration of aqueous surfactant solutions.[83–86] Quantification of monomer and monomer–alcohol mixture polarities were achieved by examination of the relative intensities of the first and third vibrational bands (I_1/I_3 ratio, ESI Fig. S2, Table S2†) of the pyrene fluorescence emission. Results obtained for

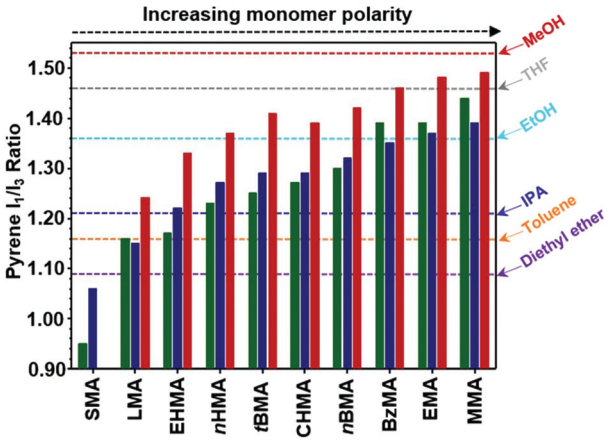

Fig. 1 Evaluation of monomer polarity by fluorescence emission spectroscopy of pyrene dissolved in various monomers and monomer–alcohol mixtures at 20 °C. Analyses conducted using pyrene dissolved in: neat methacrylate monomers (green bars), monomer–IPA mixtures (blue bars) and MeOH–monomer mixtures (red bars). Comparative analyses conducted on pyrene dissolved in neat organic solvents including: in MeOH (red dashed line), THF (grey dashed line), ethanol (cyan dashed line), IPA (blue dashed line), toluene (orange dashed line) and diethyl ether (purple dashed line).

pyrene dissolved in pure monomers showed a considerable variation in monomer polarity (Fig. 1, green bars); monomer polarity increased from SMA, the least polar monomer (I_1/I_3 = 0.95), to MMA, the most polar monomer (I_1/I_3 = 1.48). Analysis of monomer–MeOH mixtures (50 wt%) showed a significant decrease in polarity relative to neat methanol (I_1/I_3 = 1.53) for all monomers tested, with polarity decreases correlating to the polarity of the selected monomer (Fig. 1, red bars). Monomer–IPA mixtures showed different results depending upon monomer polarity relative to pure IPA (I_1/I_3 = 1.21); mixtures containing monomers less polar than IPA saw a decrease in polarity with respect to IPA whereas monomer–IPA mixtures containing more polar monomers saw considerable increases in polarity (Fig. 1, blue bars).

This highlights the range of polymerisation reaction mixture polarities which arise simply through monomer selection; for example, at a monomer concentration of 50 wt%, the I_1/I_3 ratio of an MMA–MeOH mixture (I_1/I_3 = 1.49) was comparable to that of neat methanol (I_1/I_3 = 1.53, polarity index = 5.1). In contrast the I_1/I_3 ratio obtained for the LMA–IPA mixture (I_1/I_3 = 1.15) was closer to that obtained for toluene, a solvent of considerably lower polarity (I_1/I_3 = 1.16, polarity index = 2.4). It must be noted that monomer–alcohol mixture polarities would likely decrease, from the values obtained here, at 20 °C, under typical Cu-catalysed RDRP conditions, due to the temperature dependent dielectric constant of alcohols;[87,88] this may explain initiation efficiency decreases at elevated temperature observed in our previous reports of methanolic linear polymerisations. Polarity is known to impact many polymerisation conditions, including polymerisation mixture homogeneity and catalyst solubility, and must therefore not be ignored during polymerisation design.[89,90]

Linear homopolymerisation of hydrophobic methacrylate monomers by Cu-catalysed RDRP in alcohol media at 60 °C

Homopolymerisations of hydrophobic methacrylate monomers were conducted by Cu-catalysed RDRP at 60 °C in anhydrous MeOH or anhydrous IPA (50 wt%) using a CuCl/2,2′-bipyridine (bpy) catalytic system. Benzyl 2-bromoisobutyrate (BzBiB) was selected as the initiator for all polymerisations; this greatly facilitates confirmation of monomer/initiator ratios ($[M]_0/[I]_0$) present within the polymerisation mixture before catalyst addition, monomer conversion during polymerisation, number average degree of polymerisation (DP_n) of purified polymer samples, theoretical and experimental M_n values ($M_{n(Theory)}$ and $M_{n(NMR)}$ respectively), and initiation efficiencies (IE%) by conventional ^{1}H NMR spectroscopy. BzBiB was synthesised in accordance with previously reported methods and analytical data confirmed that the correct structure had been obtained (ESI Fig. S3 and S4†).[91–93]

Polymerisations targeting a DP_n = 60 monomer units were allowed to proceed for 18 hours and were conducted in MeOH, with the exception of SMA and *t*BMA due to poor monomer–solvent miscibility and previously reported unsuccessful polymerisations respectively. During the initial stages of polymerisation all reactions appeared to proceed under controlled conditions showing the characteristic dark brown opaque homogeneous solutions commonly associated with Cu-catalysed RDRP. The polymerisations of MMA, EMA and *n*BMA remained as homogeneous solutions (Fig. 2ai) throughout the polymerisation until precipitation was observed upon cooling below 60 °C. The polymerisation of *n*HMA showed phase sep-

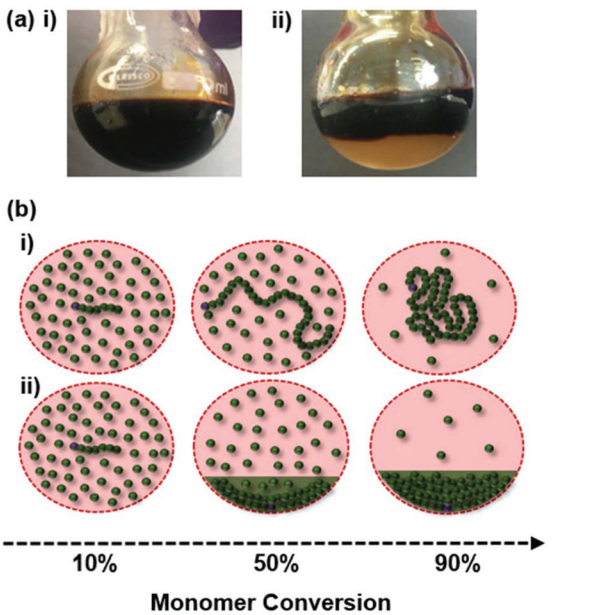

Fig. 2 Comparison of polymerisation mixture homogeneity during Cu-catalysed RDRP. (a) Photographs of polymerisations of (i) *n*BMA and (ii) EHMA after 18 hours at 60 °C in anhydrous MeOH. (b) Schematic representations of proposed co-solvency effects in (i) homogeneous and (ii) biphasic reaction mixtures.

aration during polymerisation forming a biphasic polymerisation mixture containing an opaque dark brown viscous liquid beneath a non-viscous, opaque dark brown liquid. Similar observations were made during the polymerisation of CHMA in MeOH with the polymer-containing phase forming an opaque brown solid. Conversely, BzMA, EHMA and LMA formed biphasic reaction mixtures within 3 hours of polymerisation (Fig. 2aii). The contrasting phase behaviours observed during polymerisation likely arise due to variations in monomer co-solvency during consumption and different UCST behaviours, as previously reported.[94–96] In cases where polymers display UCST behaviour in MeOH, polymers remained solvated at elevated temperature despite the loss of the monomer co-solvency effect at high conversion (Fig. 2bi). Polymers which, presumably, have phase transitions considerably above the temperatures studied here underwent phase separation during polymerisation as a diminished monomer co-solvent was no longer able to solvate growing polymer chains (Fig. 2bii).

Despite this polymerisation-induced phase separation, analysis by ^{1}H NMR surprisingly showed that all polymerisations achieved high monomer conversion (92 to >99%) after 18 hours. Analysis by triple-detection size exclusion chromatography (TD-SEC) in THF/TEA (98/2 v/v%) showed mono-modal chromatograms for all polymers (with the exception of p(LMA)) produced in MeOH, and narrow molecular weight distributions ($Đ$ = 1.12–1.26) typical of those obtained by Cu-catalysed RDRP (Table 1, ESI Fig. S8 and S9†). Analysis of Mark–Houwink–Sakurada (MHS) plots obtained for linear polymers showed α values of 0.694–0.544, representative of random coils within a theta solvent. The TD-SEC chromatogram obtained for p(LMA) displayed a broader molecular weight distribution ($Đ$ = 1.59) and a low molecular weight shoulder likely due to termination reactions during polymerisation. $M_{n(NMR)}$ values were in good agreement with $M_{n(Theory)}$ with initiation efficiencies (IE%; calculated as $[M_{n(Theory)}/M_{n(NMR)}$ or $M_{n(TD\text{-}SEC)}] \times 100\%$) ranging from 69–93%.

Polymerisations were also conducted in anhydrous IPA for a subset of monomers (Table 1b). Monomer–IPA solubility resulted in the formation of an initially homogeneous reaction mixture for SMA that was maintained during the early stages of the polymerisation; high monomer conversion was achieved after 18 hours despite the occurrence of polymerisation-induced phase separation. The purified polymer contained a relatively broad molecular weight distribution ($Đ$ = 1.53); however, $M_{n(NMR)}$ demonstrated accurate molecular weight targeting capability ($IE_{(NMR)}$ = 90%). The anhydrous MeOH and IPA polymerisations of MMA, CHMA and LMA were compared due to their varying phase behaviours under these conditions (Fig. 3).

Analysis of the refractive index (RI) and right-angle light scattering (RALS) chromatograms obtained by TD-SEC showed that the change in solvent had minimal impact on the overall polymer distribution for p(MMA) and p(CHMA) although a slight broadening was observed in anhydrous IPA reactions (ESI Fig. S10†). Considerable differences were observed between the molecular weight distributions of p(LMA) obtained by polymerisation in the different solvents (Fig. 3ci + ii). The polymerisation of LMA in MeOH yielded a polymer containing a broad molecular weight distribution ($Đ$ = 1.59) with very low initiator efficiencies ($IE_{(TD\text{-}SEC)}$ = 55%). Furthermore, the presence of a low molecular weight shoulder in the RI chromato-

Table 1 Cu-Catalysed RDRP of hydrophobic methacrylate monomers in anhydrous alcohols at 60 °C

	^{1}H NMR							TD-SEC (THF/TEA)[e]				
	$[M]_0/[I]_0$[a]	Conv. (%)[b]	$M_{n(Theory)}$[c] (g mol^{-1})	DP_n[d]	M_n[d] (g mol^{-1})	IE[d] (%)	Homogenous	M_w (g mol^{-1})	M_n (g mol^{-1})	$Đ$	IE (%)	α
(a) MeOH												
p(MMA)$_{67}$	60	99	6300	67	7000	90	Yes	11 000	9800	1.12	64	0.665
p(EMA)$_{64}$	60	97	6900	64	7600	91	Yes	10 800	8900	1.21	78	0.683
p(*n*BMA)$_{74}$	62	99	9100	74	10 800	84	Yes	13 000	11 600	1.12	72	0.690
p(*n*HMA)$_{67}$	60	>99	10 500	67	11 700	90	No	15 800	13 600	1.16	77	0.694
p(BzMA)$_{78}$[f]	60	97	10 500	—[f]	—[f]	—[f]	No	17 000	13 700	1.24	77	0.558
p(CHMA)$_{66}$	60	97	10 000	66	11 400	88	No	15 600	13 100	1.19	76	0.616
p(EHMA)$_{65}$	60	99	12 000	65	13 100	92	No	18 400	14 500	1.26	83	0.599
p(LMA)$_{80}$	60	92	14 300	80	20 600	69	No	41 400	26 000	1.59	55	0.584
(b) IPA												
p(MMA)$_{70}$	60	>99	6300	70	7300	86	Yes	11 200	9600	1.16	66	0.691
p(*t*BMA)$_{59}$	60	88	7800	59	8700	91	Yes	14 300	10 000	1.43	78	0.643
p(CHMA)$_{68}$	60	99	10 300	68	11 700	88	No	16 400	13 000	1.26	79	0.680
p(LMA)$_{66}$	60	97	15 100	66	17 000	89	No	24 400	17 800	1.37	85	0.595
p(SMA)$_{67}$	61	99	20 700	67	23 000	90	No	35 500	25 000	1.53	83	0.544

See ESI Fig. S5–S7† for details on ^{1}H NMR analyses. [a] Calculated by ^{1}H NMR analysis of polymerisation mixture at t_0. [b] Calculated by ^{1}H NMR analysis of polymerisation mixture at t_f. [c] $M_{n(Theory)} = ((([M]_0/[I]_0 \times M_{r(monomer)}) \times conv.) + M_{r(initiator)})$. [d] Calculated by ^{1}H NMR analysis of the purified polymer: $M_n = (DP_n \times M_{r(monomer)}) + M_{r(initiator)}$. [e] Calculated by TD-SEC using THF/TEA mobile phase (98/2 v/v%) at 35 °C using a flow rate of 1 mL min^{-1}. [f] Characterisation of p(BzMA$_{60}$) by ^{1}H NMR spectroscopy was not possible due to overlap between initiator and monomer resonances therefore DP_n, values were calculated using M_n values obtained by TD-SEC.

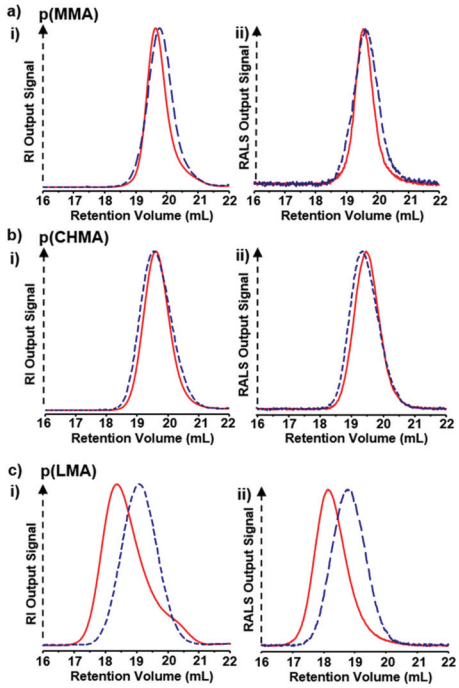

Fig. 3 Comparison of the molecular weight distributions of (a) p(MMA), (b) p(CHMA) and (c) p(LMA) generated by Cu-catalysed RDRP in MeOH (red lines) and IPA (blue dotted lines). Refractive index (i) and right angle light scattering (ii) chromatograms obtained by TD-SEC in THF/TEA (92/2 v/v%) at a flow rate of 1 mL min^{-1}.

gram (Fig. 3ci – red line) demonstrated a lack of control during the polymerisation of LMA in anhydrous methanol and suggests a level of termination. Anhydrous IPA provided an improved environment for LMA polymerisation under these conditions ($IE_{(TD\text{-}SEC)}$ = 89%) and examination of the RI chromatogram (Fig. 3ci blue dotted line) did not show the low molecular weight shoulder observed in methanol reactions.

It is possible that switching to a less polar reaction mixture may have delayed the point at which polymerisation-induced phase separation occurred thus preventing termination of oligomers in the early stages of polymerisation. The level of control observed in polymerisations varied significantly between monomers. Polymer dispersities obtained by TD-SEC showed a negative correlation with polymerisation mixture polarity (ESI Fig. S11†); it is possible that the monomer-controlled reaction polarity induces variations in the solubility of the CuCl/bpy catalytic system thus boosting the prevalence of undesirable side reactions.

Branched statistical copolymerisation with ethylene glycol dimethacrylate (EGDMA)

Having established the viability of RDRP of a range of hydrophobic methacrylate monomers in anhydrous alcohols, the synthesis of high molecular weight branched copolymer architectures was investigated for each of the most successful monomer–alcohol combinations. This was achieved by conducting Cu-catalysed RDRP in an identical manner to those described above, targeting DP_n values of 60 monomer units as previously; in addition, small amounts of ethylene glycol dimethacrylate (EGDMA) were added to generate branch points between the primary polymer chains (Scheme 1). The formation of a 3D gelled network was avoided by ensuring that the nominal ratio of EGDMA to initiator did not exceed unity ($[B]_0/[I]_0 \leq 1.00$).[97] Copolymerisations were conducted using nominal $[B]_0/[I]_0$ ratios varying from 0.59 to 0.97, as determined by ^{1}H NMR spectroscopy (ESI Fig. S12†) of the crude reaction mixtures, and were allowed to proceed for 24 hours during which the observed phase behaviours of all monomer–alcohol systems were identical to the corresponding linear polymerisations described above. Analysis of polymerisation mixtures after 24 hours showed that all polymerisations had achieved high monomer conversion (97–>99%) which is essential to promote interchain branching and facilitate the formation of high molecular weight branched polymers using this approach.[46]

Following removal of the CuCl/bpy catalytic system *via* column chromatography and subsequent purification by multiple precipitations into a suitable anti-solvent (ESI Table S3†), branched copolymers were characterised by ^{1}H NMR spectroscopy to determine DP_n and $M_{n(NMR)}$ of the constituent primary chains within the complex branched copolymer architectures (ESI Fig. S13†). Primary chain $M_{n(NMR)}$ values obtained in this way showed good agreement with $M_{n(NMR)}$ values

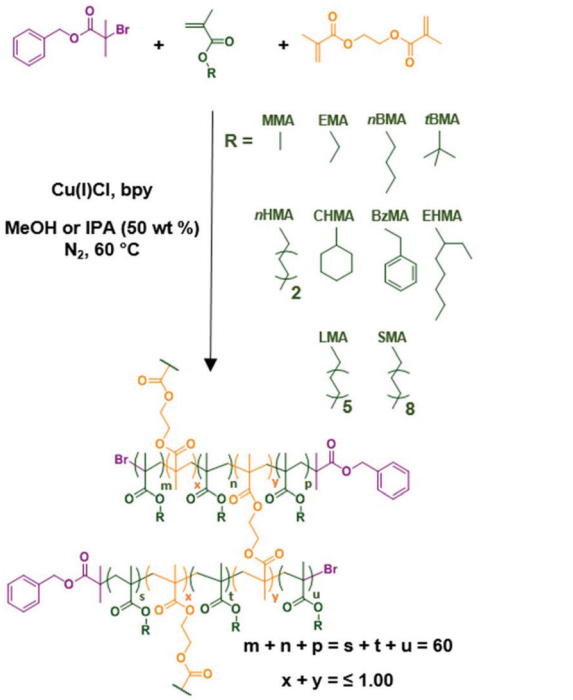

Scheme 1 Synthesis of branched statistical copolymers *via* Cu-catalysed reversible deactivated radical copolymerisation (RDRP) of hydrophobic methacrylate monomers and EGDMA in alcoholic media.

obtained for corresponding linear homologues generated in the absence of EGDMA, indicating that the presence of EGDMA has negligible impact on primary chain formation during branching copolymerisations of hydrophobic methacrylate monomers *via* alcoholic Cu-catalysed RDRP. The formation of branched copolymer architectures was confirmed by TD-SEC; in all cases, both the weight average molecular weight (M_w) and M_n values obtained by TD-SEC (M_w up to 1758 kg mol^{-1} and M_n up to 52.0 kg mol^{-1}) were significantly higher (Table 2) than those of their linear homologues (Table 1), despite agreement between DP_n values obtained by ^{1}H NMR spectroscopy. This clearly indicates the formation of branched copolymers consisting of multiple primary chains which closely resemble the linear homopolymers described above. This was accompanied by a significant decrease in α values acquired from MHS plots obtained from the branched copolymers (α = 0.378–0.471).

In all cases, overlaid MHS plots obtained for branched polymers and their linear homologues highlighted the considerable architectural differences between linear homopolymers and branched copolymers (ESI Fig. S14†).

TD-SEC chromatograms of branched copolymers also gave broad molecular weight distributions ($Đ$ = 2.09–35.08) indicating the deviation from conventional linear polymer synthesis and the considerable variety of species present within the copolymer samples created by the statistical branching process.[60] Overlays of RI and RALS chromatograms obtained by TD-SEC show these differences clearly (Fig. 4). The presence of large (high molecular weight) species was evident from the difference between chromatograms obtained. A comparison of the RI chromatogram overlays also shows very close correlation of linear homopolymers and the low molecular weight fractions of the corresponding branched statistical copolymers, indicating the presence of the component linear homopolymer primary chains within the branched copolymer distributions, as has been previously reported.[46,60] This is strongly supported by the $M_{n(NMR)}$ calculations and would suggest a near-identical number of primary chains are created in both polymerisations and that they propagate to near-identical chain lengths; molecular weight and dispersity differences are, therefore, simply due to the number and distribution of conjoined chains. The presence of unbranched primary chains is the result of the statistical nature of intermolecular branching and is an intrinsic feature of such branching copolymerisations, either due to the lack of EGDMA incorporation within all chains or consumption of incorporated EGDMA functionality *via* intramolecular cyclisation.[59,60] Unbranched linear chains were also seen within deconvoluted MHS plots where two distinct regions, consisting of either linear primary chain ($\alpha \geq$ 0.500–0.800) or branched copolymer (α < 0.500) fraction, were readily observed (ESI Fig. S15†).

The effect of varying the ratio of branching comonomer to initiator was studied across branching copolymerisations containing the various hydrophobic monomers by increasing the nominal $[B]_0/[I]_0$ ratio from 0.59 to 0.97 and comparing the resulting molecular weight distributions. In all cases, as would be expected, a significant impact on the molecular weight distributions was observed by TD-SEC (ESI Fig. S16†), with M_w, $Đ$ and the weight fraction of primary chains incorporated during branching reactions increasing. Surprisingly, the extent to which the increased EGDMA impacted the molecular weight distributions varied considerably between monomer–solvent systems. For example, in the copolymerisation of EMA and EGDMA in anhydrous MeOH, an increase in nominal $[B]_0/[I]_0$ ratio from 0.81–0.95 saw weight average molecular weights increase from 179–1485 kg mol^{-1}, whereas in the copolymerisation of SMA with EGDMA in anhydrous IPA, similar increases in nominal $[B]_0/[I]_0$ ratios resulted in modest increases in weight average molecular weights of the resultant branched copolymers from 186–352 kg mol^{-1}.

Branching copolymerisations utilising $[B]_0/[I]_0$ ratios >1.00 are expected to form insoluble gelled networks due to, crosslinking of primary chains; whilst, the branching copolymerisations described here contain nominal $[B]_0/[I]_0$ ratios ≤0.97, the varying initiation efficiencies observed in linear homopolymerisations indicate experimental $[B]_0/[I]_0$ ratios in excess of the theoretical gel point (Table 2).

Surprisingly, in many cases the formation of a gel network was avoided, and soluble branched polymers were obtained from branching copolymerisations with measured experimental $[B]_0/[I]_0$ ratios in excess of the theoretical gel point. The high monomer conversions recorded, and the absence of unreacted methacrylate groups observed during analysis of purified polymers by ^{1}H NMR spectroscopy, indicate that gel formation was not suppressed due to incomplete polymerisation of pendant methacrylate groups. It is therefore probable that in copolymerisations with experimental $[B]_0/[I]_0$ > 1.00, gelation was avoided due to the consumption of a fraction of pendant methacrylate vinyl groups (from EGDMA incorporation) *via* intramolecular cyclisation.

Comparisons between the M_w of branched copolymers with M_n values obtained for their linear equivalents (M_w(Br)/M_n(L)) provides an indication of the weight average number of chains that are conjoined during copolymerisation. Fig. 5a demonstrates the impact that experimental $[B]_0/[I]_0$ ratios has on the extent of branching; M_w(Br)/M_n(L) generally increased with experimental $[B]_0/[I]_0$ in the branching copolymerisations of EGDMA with MMA, EMA, *n*BMA, *n*HMA and EHMA. In the branching copolymerisations of the MMA–IPA and EHMA–MeOH systems, large increases in the extent of branching were observed shortly before gelation, which occurred when polymerisations were attempted at experimental $[B]_0/[I]_0$ ratios of 1.05. A similar trend was observed in branched copolymers obtained from copolymerisation of EMA with EGDMA in methanol; a sudden increase in M_w(Br)/M_n(L) occurred as experimental $[B]_0/[I]_0$ ratios were increased from 0.99 to 1.04 indicating that the latter copoylmerisation is approaching the experimental gel point. Surprisingly, similar sudden increases in the extent of branching were not observed in the copolymersations of *n*BMA and *n*HMA with EGDMA in methanol despite being conducted at experimental $[B]_0/[I]_0$ ratios of 1.12 and 1.03 respectively. This indicates that these reactions would

Table 2 Branched copolymers generated by Cu-catalysed RDRP of hydrophobic methacrylate monomers and EGDMA in anhydrous alcohols

	^{1}H NMR ($CDCl_3$) – primary chain analysis						TD-SEC (THF/TEA)[e]			
Polymer	$[M]_0/[I]_0$ [a]	$[B]_0/[I]_0$ [a]	Exp. $[B]_0/[I]_0$ [a]	Conv.[b] (%)	M_n (theory)[c] (g mol^{-1})	M_n (NMR)[d] (g mol^{-1})	M_w (kg mol^{-1})	M_n (kg mol^{-1})	$Đ$	α
(a) MeOH										
p(MMA_{67}-*co*-$EGDMA_{0.89}$)	60	0.80	0.89	Gelation observed						
p(MMA_{67}-*co*-$EGDMA_{1.00}$)	61	0.90	1.00	Gelation observed						
p(EMA_{66}-*co*-$EGDMA_{0.89}$)	59	0.81	0.89	99	7000	7800	179.3	30.0	5.97	0.384
p(EMA_{68}-*co*-$EGDMA_{0.93}$)	61	0.85	0.93	99	7200	8000	398.6	35.0	11.80	0.385
p(EMA_{67}-*co*-$EGDMA_{0.99}$)	59	0.90	0.99	99	7000	7900	538.2	44.4	17.43	0.386
p(EMA_{67}-*co*-$EGDMA_{1.04}$)	60	0.95	1.04	99	7100	7900	1485	51.6	31.78	0.415
p($n$$BMA_{70}$-*co*-$EGDMA_{0.95}$)	61	0.80	0.95	99	8900	10 200	242.2	33.4	7.25	0.393
p($n$$BMA_{73}$-*co*-$EGDMA_{1.01}$)	63	0.85	1.01	>99	9200	10 600	387.5	35.0	11.07	0.394
p($n$$BMA_{72}$-*co*-$EGDMA_{1.07}$)	63	0.90	1.07	99	9200	10 500	673.3	44.4	15.16	0.392
p($n$$BMA_{73}$-*co*-$EGDMA_{1.12}$)	62	0.94	1.12	>99	9100	10 600	798.0	51.6	15.46	0.396
p($n$$HMA_{65}$-*co*-$EGDMA_{0.87}$)	60	0.78	0.87	>99	10 500	11 300	282.6	29.5	9.58	0.383
p($n$$HMA_{67}$-*co*-$EGDMA_{0.94}$)	62	0.85	0.94	>99	10 800	11 700	530.2	41.7	12.70	0.391
p($n$$HMA_{65}$-*co*-$EGDMA_{0.98}$)	60	0.88	0.98	>99	10 400	11 300	591.1	40.9	14.45	0.389
p($n$$HMA_{68}$-*co*-$EGDMA_{1.03}$)	60	0.93	1.03	>99	10 500	11 800	981.1	50.6	19.39	0.384
p($BzMA_{78}$-*co*-$EGDMA_{0.91}$)[f]	60	0.70	0.91[f]	>99	10 800	—[f]	303.5	31.4	9.66	0.390
p($BzMA_{78}$-*co*-$EGDMA_{1.04}$)[f]	60	0.80	1.04[f]	Gelation observed						
p($BzMA_{78}$-*co*-$EGDMA_{1.17}$)[f]	60	0.90	1.17[f]	Gelation observed						
p($EHMA_{68}$-*co*-$EGDMA_{0.82}$)	62	0.75	0.82	>99	12 600	13 700	246.2	42.1	5.84	0.390
p($EHMA_{65}$-*co*-$EGDMA_{0.89}$)	60	0.82	0.89	>99	12 200	13 100	313.1	31.5	9.94	0.392
p($EHMA_{68}$-*co*-$EGDMA_{0.93}$)	63	0.86	0.93	>99	12 800	13 700	879.7	52.0	16.93	0.398
p($EHMA_{70}$-*co*-$EGDMA_{1.05}$)	64	0.97	1.05	Gelation observed						
p(LMA_{87}-*co*-$EGDMA_{1.01}$)	60	0.70	1.01	Gelation observed						
p(LMA_{87}-*co*-$EGDMA_{1.16}$)	60	0.80	1.16	Gelation observed						
p(LMA_{88}-*co*-$EGDMA_{1.30}$)	61	0.90	1.30	Gelation observed						
(b) IPA										
p(MMA_{64}-*co*-$EGDMA_{0.83}$)	56	0.71	0.83	>99	5900	6700	352.6	24.8	14.20	0.347
p(MMA_{70}-*co*-$EGDMA_{0.94}$)	62	0.81	0.94	>99	6500	7300	1758	50.1	35.08	0.382
p(MMA_{70}-*co*-$EGDMA_{1.05}$)	60	0.90	1.05	Gelation observed						
p(MMA_{70}-*co*-$EGDMA_{1.10}$)	60	0.95	1.10	Gelation observed						
p($t$$BMA_{68}$-*co*-$EGDMA_{0.77}$)	61	0.70	0.77	>99	8900	9900	66.5	31.8	2.09	0.471
p($t$$BMA_{65}$-*co*-$EGDMA_{0.93}$)	60	0.85	0.93	98	8800	9500	94.1	29.4	3.20	0.431
p($t$$BMA_{69}$-*co*-$EGDMA_{1.02}$)	63	0.93	1.02	97	9200	10 100	150.7	64.0	2.35	0.432
p($t$$BMA_{67}$-*co*-$EGDMA_{1.05}$)	60	0.96	1.05	98	8800	9800	163.2	45.3	3.60	0.422
p($CHMA_{65}$-*co*-$EGDMA_{0.67}$)	59	0.59	0.67	>99	10 200	11 200	45.5	17.3	2.34	0.415
p($CHMA_{68}$-*co*-$EGDMA_{0.91}$)	60	0.80	0.91	>99	10 400	11 700	102.9	23.5	4.38	0.403
p($CHMA_{69}$-*co*-$EGDMA_{1.03}$)	60	0.91	1.03	>99	10 400	11 900	227.1	33.5	6.70	0.391
p($CHMA_{69}$-*co*-$EGDMA_{1.06}$)	60	0.93	1.06	>99	10 400	11 900	273.2	35.6	7.68	0.398
p(LMA_{72}-*co*-$EGDMA_{0.88}$)	66	0.78	0.88	>99	17 000	18 600	96.1	32.2	2.98	0.423
p(LMA_{65}-*co*-$EGDMA_{0.96}$)	60	0.85	0.96	>99	15 500	16 800	111.1	33.4	3.32	0.407
p(LMA_{64}-*co*-$EGDMA_{1.01}$)	59	0.90	1.01	>99	15 300	16 500	147.1	30.2	4.86	0.402
p(LMA_{70}-*co*-$EGDMA_{1.04}$)	64	0.93	1.04	>99	16 500	18 100	294.4	54.0	5.46	0.386
p(SMA_{72}-*co*-$EGDMA_{0.89}$)	64	0.80	0.89	>99	21 900	24 700	186.0	43.5	4.27	0.404
P(SMA_{73}-*co*-$EGDMA_{0.96}$)	65	0.85	0.94	>99	22 200	24 900	208.0	39.6	5.24	0.399
p(SMA_{68}-*co*-$EGDMA_{1.00}$)	62	0.90	1.00	>99	21 200	23 300	362.6	43.1	8.83	0.376
p(SMA_{65}-*co*-$EGDMA_{1.06}$)	60	0.95	1.06	>99	20 600	22 300	352.4	53.1	6.63	0.392

[a] Calculated by ^{1}H NMR spectroscopy of polymerisation mixture at t_0. [b] Calculated by ^{1}H NMR spectroscopy of polymerisation mixture at t_f. [c] $M_{n(Theory)} = (([M]_0/[I]_0 \times M_{r(monomer)}) \times conv.) + M_{r(Initiator)})$. [d] Calculated by ^{1}H NMR spectroscopy of the purified polymer: $M_{n(PC)} = (DP_n \times M_{r(monomer)}) + M_{r(initiator)}$. [e] Calculated by TD-SEC using THF/TEA mobile phase (98/2 v/v%) at 35 °C using a flow rate of 1 mL min^{-1}. [f] Characterisation of p($BzMA_{60}$-*co*-$EGDMA_{0.70}$) by ^{1}H NMR spectroscopy was not possible due to overlap between initiator and monomer resonances.

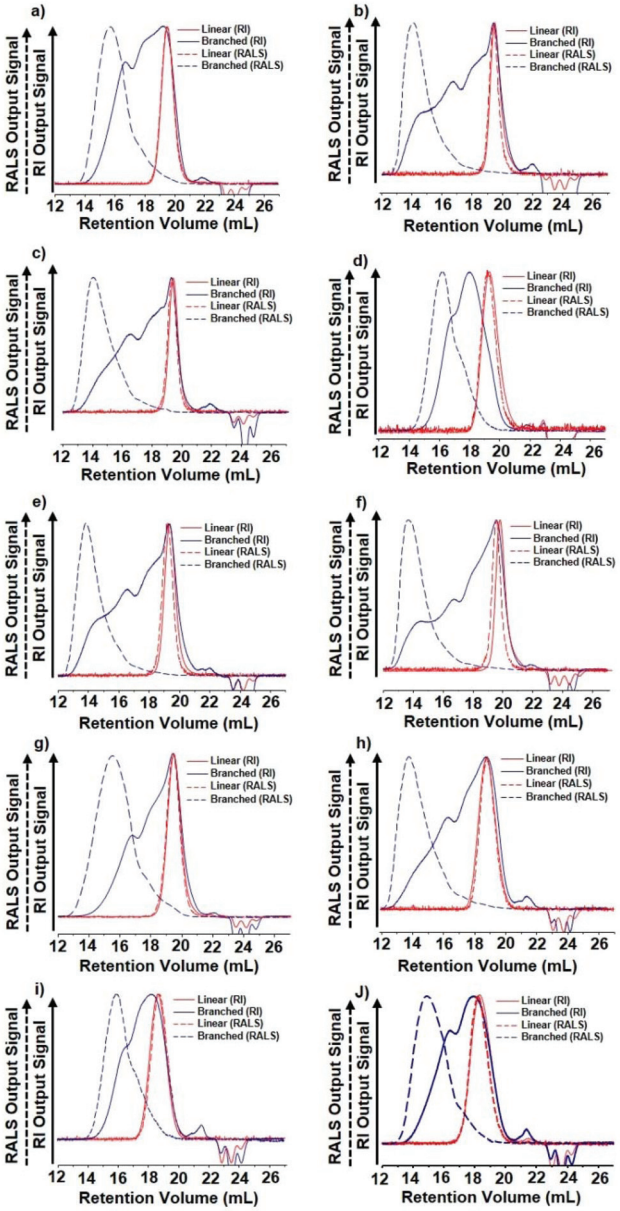

Fig. 4 Comparison of molecular weight distributions obtained by TD-SEC. Overlaid refractive index (RI; solid lines) and right-angle light scattering (RALS; dotted lines) chromatograms obtained for linear homopolymers (red, Table 1) and the highest molecular weight branched statistical copolymers (blue, Table 2) obtained for the following monomer–alcohol systems: (a) MMA–IPA, (b) EMA–MeOH (c) *n*BMA–MeOH, (d) *t*BMA–IPA, (e) *n*HMA–MeOH (f) BzMA–MeOH, (g) CHMA–IPA, (h) EHMA–MeOH, (i) LMA–IPA and (j) SMA–IPA.

likely tolerate experimental $[B]_0/[I]_0$ greater than those reported here before the onset of gelation. The extent of branching observed in the copolymerisations of EGDMA with *t*BMA, CHMA, LMA or SMA were significantly lower than those described above. The CHMA/EGDMA reaction was studied across a wide range of experimental $[B]_0/[I]_0$ ratios ranging from 0.67 to 1.06 which gave increased $M_w(Br)/M_n(L)$ from 2.77 to 16.66 chains. Much smaller differences in the extent of branching were recorded for the LMA/EGDMA and SMA/EGDMA systems. Copolymerisations of LMA with EGDMA at experimental $[B]_0/[I]_0$ ratios ranging from 0.88 to 1.04 resulted in an increase in the observed $M_w(Br)/M_n(L)$ from 3.94 to 12.07 chains. Similar increases were observed in the SMA/EGDMA copolymerisation where $M_w(Br)/M_n(L)$ increased from 5.24 to 9.93 chains as experimental $[B]_0/[I]_0$ ratios were raised from 0.89 to 1.06. The disparity in the extent of branching observed was surprising and indicated varying contributions of intermolecular branching and intramolecular cyclisation during copolymerisation in the different monomer/EGDMA systems.

Analyses of the cumulative weight fraction (ω_i) *versus* absolute molecular weight, for the highest molecular weight branched copolymers obtained from each of the monomer–alcohol systems, were conducted to account for the M_n of the primary chains from which each macromolecule is constructed (ESI eqn (S1),† Fig. 5b). This analysis unveils the impact of varying repeat unit mass, and therefore structure, on the resulting molecular weights obtained (as judged by TD-SEC analysis), and provides insight into the contribution of each branched species within the distribution of each sample.

The extent of branching within the samples studied follow the order of EMA > MMA > *n*BMA ≈ *n*HMA > EHMA ≫ CHMA > BzMA > LMA > *t*BMA > SMA which supports the $M_w(Br)/M_n(L)$ analyses described above. This trend was reaffirmed when similar analyses were conducted using the cumulative mole fraction (ESI Fig. S17†). It must be stated however that the samples studied were generated using varied experimental $[B]_0/[I]_0$ ratios therefore the ordering identified is only relevant to the samples described here and is not indicative of branching efficacy between monomer/EGDMA systems.

This analysis was used to further demonstrate the discrepancy between copolymerisations which exhibited high and low levels of branching. The composition of branched copolymers possessing the highest weight average molecular weights, prepared by copolymerisation of EMA and SMA with EGDMA in methanol and IPA respectively, contained comparable chain lengths and EGDMA content as determined by ^{1}H NMR. However, analysis of p(EMA$_{67}$-*co*-EGDMA$_{1.04}$) and p(SMA$_{65}$-*co*-EGDMA$_{1.06}$) by TD-SEC showed a large contrast in the level of branching observed in branched copolymer samples. Analysis showed that the lowest 25% of the cumulative weight fraction (ω_i = 0.25) was made up of branched copolymers containing no more than 4 and 2 primary chains in p(EMA$_{66}$-*co*-EGDMA$_{1.04}$) and p(SMA$_{65}$-*co*-EGDMA$_{1.06}$) respectively. In contrast the same analysis showed that 75% of the weight fraction (ω_i = 0.75) was made up polymer chains containing up to 104 and 15 chains respectively; the upper quartile of the p(EMA$_{66}$-*co*-EGDMA$_{1.04}$) molecular weight distribution therefore has >7-fold higher number of conjoined chains than p(SMA$_{65}$-*co*-EGDMA$_{1.06}$) (Fig. 5c).

This can be explained by three key differences which arise, and likely influence, branching reactions during varying copolymerisations which target the same weight% solids content and the same primary chain DP$_n$. Most strikingly, the active chain-end concentration, within the MMA to SMA copolymeri-

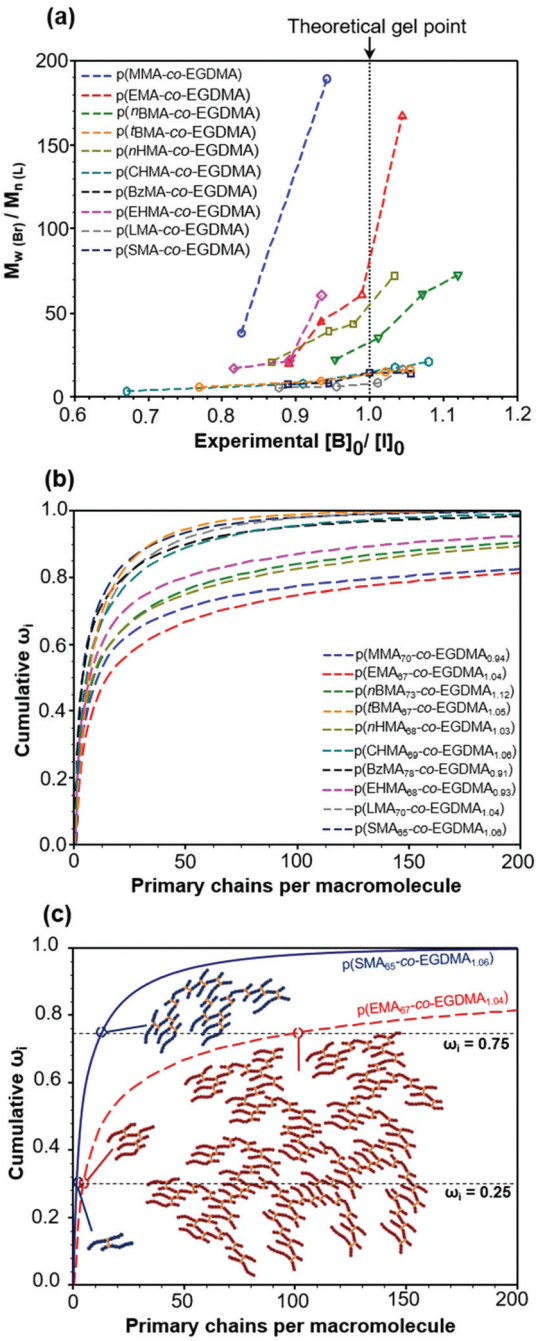

Fig. 5 Analysis of branched copolymers produced by Cu-catalysed statistical RDRP of methacrylate monomers with EGDMA using TD-SEC. (a) Graphical representation of the impact of experimental $[B]_0/[I]_0$ ratios on the molecular weights of branched copolymers relative to those of their linear homologues, M_w(Br)/M_n(L). (b) Plots showing the contributions of each branched species towards the cumulative ω_i for branched copolymers possessing the highest M_w from each monomer/EGDMA system. (c) A comparison showing the variation in the extent of branching in branched copolymer species which make up 0.25 and 0.75 of the cumulative ω_i in p(EMA$_{68}$-*co*-EGDMA$_{1.04}$) (red) and p(SMA$_{65}$-*co*-EGDMA$_{1.06}$) (blue).

sation series, decreases significantly when seeking to achieve constant solids content and identical chain length; the monomer molecular weight increase across the series can also be considered as a vinyl group weight fraction within the monomers as decreasing from 85 wt% to 25 wt% which necessitates a subsequent reduction in initiator concentration to target a fixed DP_n (Fig. 6a, ESI Table S4†). A normalised active chain-end concentration factor can be calculated for each branching copolymerisation studied; across the extremes of the copolymerisations reported here, active chain-end concentrations for an MMA/EGDMA branched copolymerisation is 3.38-fold higher than the equivalent SMA/EGDMA reaction. The impact of polymerisation concentration on the prevalence of intramolecular cyclisation is well known and can likely explain the relatively low levels of branching observed in the copolymerisations of LMA and SMA with EGDMA, compared with those conducted under similar experimental $[B]_0/[I]_0$ ratios, at higher active chain-end concentrations. Additionally, the variation in steric hindrance created by the methacrylate side-chain must also be considered; as the polymer pendant groups increase in size, the side chains will ultimately exceed the length of the pendant vinyl groups resulting from EGDMA incorporation (Fig. 6b). Molecular modelling calculations show that the pendant methacrylate group of an EGDMA repeat unit protrudes an average distance of 0.889 nm from the primary chain backbone; repeat unit side chains of MMA and LMA protrude a distance of 0.427 nm and 1.619 nm respectively (Fig. 5b, ESI Fig. S18, Table S6†). Whilst this highlights the increasing steric hindrance to incoming radicals, it is unclear whether this would actually promote consumption of pendant methacrylate groups *via* intramolecular cyclisation over intermolecular branching reactions.[98]

Finally, the varying solvent environment within these polymerisations, and the impact on the phase behaviour of the branched copolymers during propagation, may also be important. This may be highly specific to the alcoholic copolymerisations discussed above, however, we have previously hypothesised that in polymerisations where monomer consumption progressively changes the solvent environment within the reaction mixture, the formation of densely coiled structures is likely.[80,82] In the branching copolymerisations described here, it is likely that significant differences in the conformations of the propagating primary chains within highly branched structures and the lightly branched fraction across the copolymerising monomer series exist (Fig. 6c). Branching copolymerisations of MMA with EGDMA gave homogeneous reactions mixtures, even after cooling, indicating that branched copolymers remained well solvated throughout polymerisation. In contrast, *n*BMA/EGDMA branching copolymerisations were homogeneous until heating was withdrawn and *n*HMA/EGDMA copolymerisations remained homogenous until high monomer conversion. It is reasonable to envisage that in relatively poor solvent environments, branched copolymers will adopt densely packed conformations, reducing the availability of pendant methacrylate groups and reducing the overlap between chain dimensions in solution; this would additionally hinder successful intermolecular branching. Several of monomer/EGDMA copolymerisations studied formed biphasic reaction mixtures during copolymerisation, giving distinct and

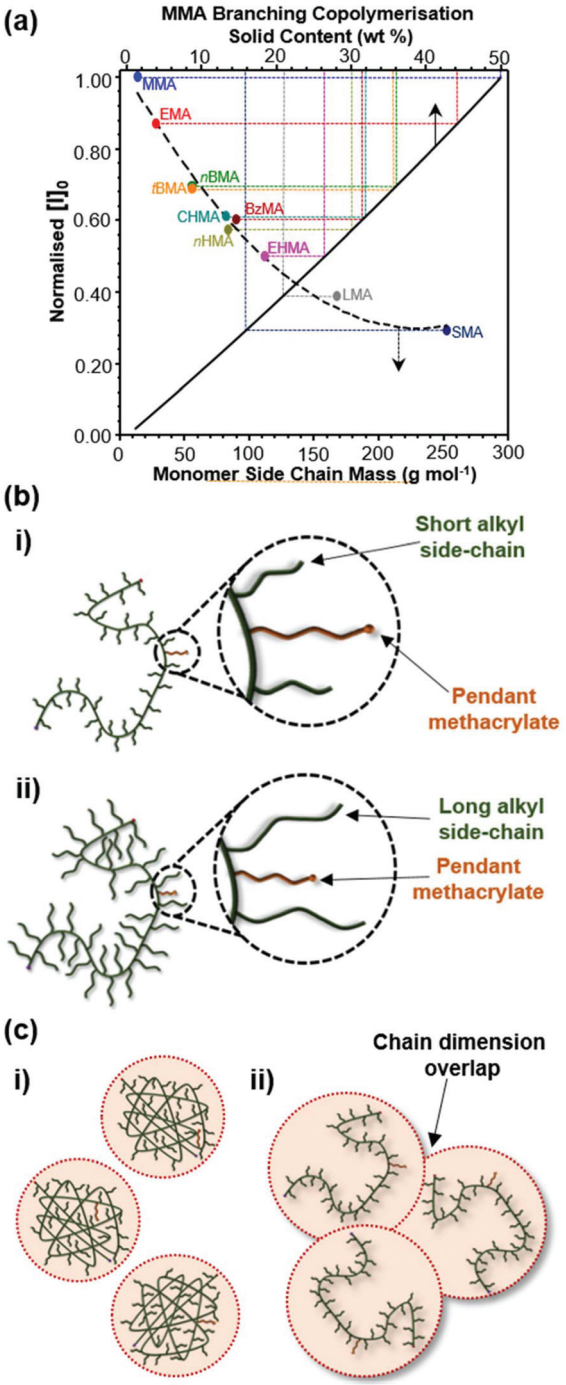

Fig. 6 Factors affecting branching in the copolymerisation of hydrophobic methacrylates with EGDMA *via* Cu-catalysed RDRP in alcohols. (a) The inherent concentration factor which arises with increasing monomer side chain length during branching copolymerisations conducted at a concentration of 50 wt%. (b) Schematic representation of the steric hindrance around pendant methacrylate groups in the presence of monomers containing (i) short and (ii) long alkyl side chains. (c) Schematic representation of proposed primary chain conformations in different solvent environments. (i) Collapsed polymer chains within a bad solvent environment and (ii) expanded polymer chains within a good solvent environment.

highly viscous polymer-rich phases. It is likely that the varied phase behaviours, and assumed associated conformational changes, negatively impact the creation of intermolecular branches; this is somewhat supported by the high levels of branching observed for MMA/EGDMA and EMA/EGDMA systems in contrast to lower branching levels seen in the *n*BMA/EGDMA and *n*HMA/EGDMA systems. The lowest degrees of branching were observed in copolymerisations of CHMA, LMA and SMA, which form biphasic reaction mixtures in the early stages of polymerisation with subsequent suppression of branching.

Conclusions

In this work we aimed to expand the scope of Cu-catalysed RDRP of hydrophobic methacrylate monomers in alcoholic solvents and explore the viability of the synthesis of a range of branched polymer architectures using this unconventional approach.

An attraction of RDRP reactions is the ability to conduct controlled polymerisations at high solids contents, leading to final polymer solutions of >50% w/w; however, it is clear that monomer selection has the potential to impact the initial solvent environment, whilst monomer depletion during propagation, and formation of polymer, may lead to a transition from a "good" solvent environment to a "poor" solvent condition, as exploited by the so-called polymerization-induced self-assembly, or PISA, reactions.[71] Equally, varying solvent/monomer mixture polarity may also impact the solubility of the catalytic systems employed and alterations of the reversible-deactivation equilibrium during different stages of polymerisation. These effects are readily overlooked within reactions where the reaction solvent is a good solvent for all reaction components and products. We have seen that homogeneity is not a critical parameter in many of these polymerisations and the delayed onset of phase-separation, likely due to monomer co-solvency, does not appear to have a considerable impact on the achievement of high conversions or low $Đ$ values. Further work, to determine catalyst solubility within different monomer–solvent mixtures as well as kinetic monitoring of Cu-catalysed RDRP of hydrophobic monomers in alcoholic media, are ongoing.

The ability to conduct Cu-catalysed RDRP in anhydrous methanol and IPA across a range of hydrophobic monomers from methyl to stearyl methacrylate, including cyclic aromatic/aliphatic and branched alkyl side chains, is remarkable; the low dispersity and molecular weight targeting to give linear homopolymers is highly interesting with value potentially in more environmentally favourable solvent systems being employed on large scales. Additionally, incorporation of EGDMA at low co-monomer concentrations, was not unduly impacted and offers a readily available route to the formation of branched vinyl polymers; to the best of the authors' knowledge, this is the first report on the preparation of branched statistical copolymers containing either *n*HMA, CHMA, BzMA,

EHMA, LMA or SMA using Cu-catalysed RDRP in alcoholic media. Again, further studies are required to optimise branching copolymerisations of this type under these conditions, but it may be possible to overcome poor branching efficacies through simple changes to experimental design, including: incremental increases to the $[B]_0/[I]_0$ ratios beyond those studied here to establish the experimental gel point, varying the chemistry and chain length of the BFM used (to overcome inter-chain steric issues) and variations in reaction solids content and subsequent initial solvent environment.

Conflicts of interest

There are no conflicts to declare.

Acknowledgements

The authors would like to thank the Engineering and Physical Sciences Research Council for funding that aided this research (EP/L02635X/1 and EP/R010544/1). SF is grateful for a PhD studentship and would also like to acknowledge the John Lennon Memorial Scholarship for financial support during his PhD studies. The University of Liverpool and Materials Innovation Factory are gratefully acknowledged for access to analytical techniques and equipment.

Notes and references

1 A. Sandeau, S. Mazières and M. Destarac, *Polymer*, 2012, **53**, 5601–5618.
2 K. Matyjaszewski and N. V. Tsarevsky, *J. Am. Chem. Soc.*, 2014, **136**, 6513–6533.
3 H. Bergenudd, G. Coullerez, M. Jonsson and E. Malmström, *Macromolecules*, 2009, **42**, 3302–3308.
4 W. A. Braunecker and K. Matyjaszewski, *Prog. Polym. Sci.*, 2007, **32**, 93–146.
5 T. Otsu, Y. Takayuki and T. Masatoshi, *Makromol. Chem., Rapid Commun.*, 1982, **3**, 133–140.
6 C. J. Hawker, J. M. J. Frechet, R. B. Grubbs and J. Dao, *J. Am. Chem. Soc.*, 2005, **117**, 10763–10764.
7 G. Moad and E. Rizzardo, *Macromolecules*, 1995, **28**, 8722–8728.
8 M. K. Georges, R. P. N. Veregin, P. M. Kazmaier and G. K. Hamer, *Macromolecules*, 1993, **26**, 2987–2988.
9 C. J. Hawker, G. G. Barclay and J. Dao, *J. Am. Chem. Soc.*, 1996, **118**, 11467–11471.
10 M. Kato, M. Kamigaito, M. Sawamoto and T. Higashimura, *Macromolecules*, 1995, **28**, 1721–1723.
11 K. Matyjaszewski and J. Wang, *J. Am. Chem. Soc.*, 1995, **117**, 5614–5615.
12 K. Matyjaszewski, S. Gaynor and J. S. Wang, *Macromolecules*, 1995, **28**, 2093–2095.
13 H. Han and N. V. Tsarevsky, *Chem. Sci.*, 2014, **5**, 4599–4609.
14 J. Jeffery, F. Ercole, R. T. A. Mayadunne, G. Moad, E. Rizzardo, T. P. T. Le, J. Chiefari, J. Krstina, Y. K. (Bill) Chong, C. L. Moad, S. H. Thang and G. F. Meijs, *Macromolecules*, 2002, **31**, 5559–5562.
15 V. Percec, T. Guliashvili, J. S. Ladislaw, A. Wistrand, A. Stjerndahl, M. J. Sienkowska, M. J. Monteiro and S. Sahoo, *J. Am. Chem. Soc.*, 2006, **128**, 14156–14165.
16 D. A. Z. Wever, P. Raffa, F. Picchioni and A. A. Broekhuis, *Macromolecules*, 2012, **45**, 4040–4045.
17 A. Mühlebach, S. G. Gaynor and K. Matyjaszewski, *Macromolecules*, 1998, **31**, 6046–6052.
18 R. Nicolaÿ, Y. Kwak and K. Matyjaszewski, *Chem. Commun.*, 2008, 5336–5338.
19 F. Alsubaie, A. Anastasaki, P. Wilson and D. M. Haddleton, *Polym. Chem.*, 2015, **6**, 406–417.
20 L. Martin, G. Gody and S. Perrier, *Polym. Chem.*, 2015, **6**, 4875–4886.
21 G. Gody, R. Barbey, M. Danial and S. Perrier, *Polym. Chem.*, 2015, **6**, 1502–1511.
22 C. Boyer, A. Derveaux, P. B. Zetterlund and M. R. Whittaker, *Polym. Chem.*, 2012, **3**, 117–123.
23 G. Gody, T. Maschmeyer, P. B. Zetterlund and S. Perrier, *Macromolecules*, 2014, **47**, 3451–3460.
24 A. Kuroki, I. Martinez-Botella, C. H. Hornung, L. Martin, E. G. L. Williams, K. E. S. Locock, M. Hartlieb and S. Perrier, *Polym. Chem.*, 2017, **8**, 3249–3254.
25 N. G. Engelis, A. Anastasaki, R. Whitfield, G. R. Jones, E. Liarou, V. Nikolaou, G. Nurumbetov and D. M. Haddleton, *Macromolecules*, 2018, **51**, 336–342.
26 N. G. Engelis, A. Anastasaki, G. Nurumbetov, N. P. Truong, V. Nikolaou, A. Shegiwal, M. R. Whittaker, T. P. Davis and D. M. Haddleton, *Nat. Chem.*, 2017, **9**, 171–178.
27 J. Hu, R. Qiao, M. R. Whittaker, J. F. Quinn and T. P. Davis, *Aust. J. Chem.*, 2017, **70**, 1161–1170.
28 R. Whitfield, A. Anastasaki, N. P. Truong, P. Wilson, K. Kempe, J. A. Burns, T. P. Davis and D. M. Haddleton, *Macromolecules*, 2016, **49**, 8914–8924.
29 S. Averick, A. Simakova, S. Park, D. Konkolewicz, A. J. D. Magenau, R. A. Mehl and K. Matyjaszewski, *ACS Macro Lett.*, 2012, **1**, 6–10.
30 J. Rosselgong, E. G. L. Williams, T. P. Le, F. Grusche, T. M. Hinton, M. Tizard, P. Gunatillake and S. H. Thang, *Macromolecules*, 2013, **46**, 9181–9188.
31 D. Boschmann and P. Vana, *Macromolecules*, 2007, **40**, 2683–2693.
32 H. Chaffey-Millar, M. H. Stenzel, T. P. Davis, M. L. Coote and C. Barner-Kowollik, *Macromolecules*, 2006, **39**, 6406–6419.
33 R. Aksakal, M. Resmini and C. R. Becer, *Polym. Chem.*, 2016, **7**, 171–175.
34 R. M. England and S. Rimmer, *Polym. Chem.*, 2010, **1**, 1533–1544.
35 J. J. Hobson, S. Edwards, R. A. Slater, P. Martin, A. Owen and S. P. Rannard, *RSC Adv.*, 2018, **8**, 12984–12991.
36 B. Liu, A. Kazlauciunas, J. T. Guthrie and S. Perrier, *Macromolecules*, 2005, **38**, 2131–2136.

37 B. Liu, A. Kazlauciunas, J. T. Guthrie and S. Perrier, *Polymer*, 2005, **46**, 6293–6299.
38 Q. Ren, F. Gong, C. Liu, G. Zhai, B. Jiang, C. Liu and Y. Chen, *Eur. Polym. J.*, 2006, **42**, 2573–2580.
39 T. Zhao, Y. Zheng, J. Poly and W. Wang, *Nat. Commun.*, 2013, **4**, 1–8.
40 W. Wang, Y. Zheng, E. Roberts, C. J. Duxbury, L. Ding, D. J. Irvine and S. M. Howdle, *Macromolecules*, 2007, **40**, 7184–7194.
41 W. Du, A. M. Nyström, L. Zhang, K. T. Powell, Y. Li, C. Cheng, S. A. Wickline and K. L. Wooley, *Biomacromolecules*, 2008, **9**, 2826–2833.
42 S. Li, J. Han and C. Gao, *Polym. Chem.*, 2013, **4**, 1774–1787.
43 J. A. Alfurhood, H. Sun, P. R. Bachler and B. S. Sumerlin, *Polym. Chem.*, 2016, **7**, 2099–2104.
44 J. A. Alfurhood, P. R. Bachler and B. S. Sumerlin, *Polym. Chem.*, 2016, **7**, 3361–3369.
45 F. Isaure, P. A. G. Cormack, S. Graham, D. C. Sherrington, S. P. Armes and V. Bütün, *Chem. Commun.*, 2004, **4**, 1138–1139.
46 I. Bannister, N. C. Billingham, S. P. Armes, S. P. Rannard and P. Findlay, *Macromolecules*, 2006, **39**, 7483–7492.
47 I. Bannister, N. C. Billingham and S. P. Armes, *Soft Matter*, 2009, **5**, 3495–3504.
48 Q. Yu, S. Xu, H. Zhang, Y. Ding and S. Zhu, *Polymer*, 2009, **50**, 3488–3494.
49 I. M. R. Trigo, M. A. D. Conçalves, R. C. S. Dias and M. R. P. F. N. Costa, *Macromol. Symp.*, 2008, **271**, 107–119.
50 S. Liang, X. Li, W. J. Wang, B. G. Li and S. Zhu, *Macromolecules*, 2016, **49**, 752–759.
51 Y. Li and S. P. Armes, *Macromolecules*, 2005, **38**, 8155–8162.
52 J. C. Hernández-Ortiz, E. Vivaldo-Lima, L. M. F. Lona, N. T. McManus and A. Penlidis, *Macromol. React. Eng.*, 2009, **3**, 288–311.
53 D. J. Krasznai, T. F. L. McKenna, M. F. Cunningham, P. Champagne and N. M. B. Smeets, *Polym. Chem.*, 2012, **3**, 992–1001.
54 N. M. B. Smeets, *Eur. Polym. J.*, 2013, **49**, 2528–2544.
55 H. Yang, Z. Wang, Y. Zheng, W. Huang, X. Xue and B. Jiang, *Polym. Chem.*, 2017, **8**, 2137–2144.
56 C. D. Vo, J. Rosselgong, S. P. Armes and N. C. Billingham, *Macromolecules*, 2007, **40**, 7119–7125.
57 N. Ide and T. Fukuda, *Macromolecules*, 1999, **32**, 95–99.
58 J. Rosselgong, S. P. Armes, W. Barton and D. Price, *Macromolecules*, 2009, **42**, 5919–5924.
59 W. Huang, H. Yang, X. Xue, B. Jiang, J. Chen, Y. Yang, H. Pu, Y. Liu, D. Zhang, L. Kong and G. Zhai, *Polym. Chem.*, 2013, **4**, 3204–3211.
60 X. Xue, Y. Wang, W. Huang, H. Yang, J. Chen, J. Fang, Y. Yang, L. Kong and B. Jiang, *Macromol. Chem. Phys.*, 2015, **216**, 1555–1561.
61 J. Rosselgong, S. P. Armes, W. R. S. Barton and D. Price, *Macromolecules*, 2010, **43**, 2145–2156.
62 W. Li, J. A. Yoon, M. Zhong and K. Matyjaszewski, *Macromolecules*, 2011, **44**, 3270–3275.
63 J. Rosselgong and S. P. Armes, *Macromolecules*, 2012, **45**, 2731–2737.
64 J. Rosselgong and S. P. Armes, *Polym. Chem.*, 2015, **6**, 1143–1149.
65 A. Moreno, S. Grama, T. Liu, M. Galià, G. Lligadas and V. Percec, *Polym. Chem.*, 2017, **8**, 7559–7574.
66 M. Enayati, R. L. Jezorek, R. B. Smail, M. J. Monteiro and V. Percec, *Polym. Chem.*, 2016, **7**, 5930–5942.
67 R. L. Jezorek, M. Enayati, R. B. Smail, J. Lejnieks, S. Grama, M. J. Monteiro and V. Percec, *Polym. Chem.*, 2017, **8**, 3405–3424.
68 M. Enayati, R. B. Smail, S. Grama, R. L. Jezorek, M. J. Monteiro and V. Percec, *Polym. Chem.*, 2016, **7**, 7230–7241.
69 S. Grama, J. Lejnieks, M. Enayati, R. B. Smail, L. Ding, G. Lligadas, M. J. Monteiro and V. Percec, *Polym. Chem.*, 2017, **8**, 5865–5874.
70 R. B. Smail, R. L. Jezorek, J. Lejnieks, M. Enayati, S. Grama, M. J. Monteiro and V. Percec, *Polym. Chem.*, 2017, **8**, 3102–3123.
71 N. J. Warren and S. P. Armes, *J. Am. Chem. Soc.*, 2014, **136**, 10174–10185.
72 Z. Ding, C. Gao, S. Wang, H. Liu and W. Zhang, *Polym. Chem.*, 2015, **6**, 8003–8011.
73 Z. Song, X. He, C. Gao, H. Khan, P. Shi and W. Zhang, *Polym. Chem.*, 2015, **6**, 6563–6572.
74 J. Jennings, G. He, S. M. Howdle and P. B. Zetterlund, *Chem. Soc. Rev.*, 2016, **45**, 5055–5084.
75 M. J. Derry, L. A. Fielding and S. P. Armes, *Prog. Polym. Sci.*, 2016, **52**, 1–18.
76 N. J. W. Penfold, J. R. Lovett, N. J. Warren, P. Verstraete, J. Smets and S. P. Armes, *Polym. Chem.*, 2016, **7**, 79–88.
77 T. Cuneo, R. W. Graff, X. Wang and H. Gao, *Macromol. Chem. Phys.*, 2019, **1800546**, 1–8.
78 R. W. Graff, X. Wang and H. Gao, *Macromolecules*, 2015, **48**, 2118–2126.
79 K. Min and H. Gao, *J. Am. Chem. Soc.*, 2012, **134**, 15680–15683.
80 A. B. Dwyer, P. Chambon, A. Town, T. He, A. Owen and S. P. Rannard, *Polym. Chem.*, 2014, **5**, 3608–3616.
81 F. Y. Hern, A. Hill, A. Owen and S. P. Rannard, *Polym. Chem.*, 2018, **9**, 1767–1771.
82 A. B. Dwyer, P. Chambon, A. Town, F. L. Hatton, J. Ford and S. P. Rannard, *Polym. Chem.*, 2015, **6**, 7286–7296.
83 D. C. Dong and M. A. Winnik, *Photochem. Photobiol.*, 1982, **35**, 17–21.
84 V. Glushko, M. S. R. Thaler and C. D. Karp, *Arch. Biochem. Biophys.*, 1981, **210**, 33–42.
85 L. Piñeiro, M. Novo and W. Al-Soufi, *Adv. Colloid Interface Sci.*, 2015, **215**, 1–12.
86 E. D. Goddard, N. J. Turro, P. L. Kuo and K. P. Ananthapadmanabhan, *Langmuir*, 2005, **1**, 352–355.
87 A. C. Galvão, W. S. Robazza, G. N. Sarturi, F. C. Goulart and D. Conte, *J. Chem. Eng. Data*, 2016, **61**, 2997–3002.
88 A. Chaudhari, P. Khirade, R. Singh, S. N. Helambe, N. K. Narain and S. C. Mehrotra, *J. Mol. Liq.*, 1999, **82**, 245–253.

89 M. Horn and K. Matyjaszewski, *Macromolecules*, 2013, **46**, 3350–3357.
90 Z. C. Chen, C. L. Chiu and C. F. Huang, *Polymers*, 2014, **6**, 2552–2572.
91 M. Long, D. W. Thornthwaite, S. H. Rogers, G. Bonzi, F. R. Livens and S. P. Rannard, *Chem. Commun.*, 2009, 6406–6408.
92 M. Long, S. H. Rogers, D. W. Thornthwaite, F. R. Livens and S. P. Rannard, *Polym. Chem.*, 2011, **2**, 581–588.
93 M. Long, D. W. Thornthwaite, S. H. Rogers, F. R. Livens and S. P. Rannard, *Polym. Chem.*, 2012, **3**, 154–161.
94 Q. Zhang and R. Hoogenboom, *Prog. Polym. Sci.*, 2015, **48**, 122–142.
95 C. Pietsch, R. Hoogenboom and U. S. Schubert, *Polym. Chem.*, 2010, **1**, 1005–1008.
96 J. H. Liu, U. Wais, Y. M. Zuo, Y. Xiang, Y. H. Wang, A. W. Jackson, T. He and H. Zhang, *J. Mater. Chem. B*, 2017, **5**, 423–427.
97 A. R. Wang and S. Zhu, *Polym. Eng. Sci.*, 2005, **45**, 720–727.
98 H. Cauldbeck, M. Le Hellaye, M. Long, S. M. Kennedy, R. L. Williams, V. R. Kearns and S. P. Rannard, *J. Controlled Release*, 2016, **244**, 41–51.